



LAWRENCE  
LIVERMORE  
NATIONAL  
LABORATORY

# The feasibility of bomb radiocarbon analysis to support an age-at-length relationship for red abalone, *Haliotis rufescens* Swainson in northern California

R. T. Leaf, A. H. Andrews, G. M. Cailliet, T. A. Brown

January 7, 2009

Journal of Shellfish Research

## **Disclaimer**

---

This document was prepared as an account of work sponsored by an agency of the United States government. Neither the United States government nor Lawrence Livermore National Security, LLC, nor any of their employees makes any warranty, expressed or implied, or assumes any legal liability or responsibility for the accuracy, completeness, or usefulness of any information, apparatus, product, or process disclosed, or represents that its use would not infringe privately owned rights. Reference herein to any specific commercial product, process, or service by trade name, trademark, manufacturer, or otherwise does not necessarily constitute or imply its endorsement, recommendation, or favoring by the United States government or Lawrence Livermore National Security, LLC. The views and opinions of authors expressed herein do not necessarily state or reflect those of the United States government or Lawrence Livermore National Security, LLC, and shall not be used for advertising or product endorsement purposes.

1 TITLE

2 The feasibility of bomb radiocarbon analysis to support an age-at-length relationship for red  
3 abalone, *Haliotis rufescens* Swainson in northern California

5 RUNNING TITLE

6 Bomb  $^{14}\text{C}$  and red abalone age and growth

8 *Abstract:* Analysis of bomb generated radiocarbon ( $^{14}\text{C}$ ) changes in a red abalone, *Haliotis*  
9 *rufescens* Swainson shell was used to investigate age-at-length relationships derived from data  
10 from a previous multi-year, multi-site tag-recapture study. Shell carbonate was extracted from four  
11 successive growth trajectory locations in a single shell with a length of 251 mm MSL. Extraction  
12 locations were based on VBGF predictions and chosen to span the initial rise of the  $^{14}\text{C}$ -bomb  
13 pulse that is known to have occurred in surface ocean waters during  $1958 \pm 1$  y in the northeast  
14 Pacific. The close temporal correspondence of the red abalone sample series to regional  $\Delta^{14}\text{C}$   
15 records demonstrated the utility of the technique for validating age-at-length relationships for the  
16 red abalone. The findings provided support for a mean VBGF derived age of 32 y (range 30 to 33  
17 y) for the specimen; however, the analysis of  $^{14}\text{C}$  data indicated that the specimen could be older.

19 Key Words: accelerator mass spectrometry, carbon-14, von Bertalanffy growth function,  
20 Haliotidae

22 Authors:

23 Robert T. Leaf\*, Allen H. Andrews, Gregor M. Cailliet  
24 Moss Landing Marine Laboratories  
25 8272 Moss Landing Road  
26 Moss Landing, CA 95039

28 Thomas A. Brown  
29 Center for Accelerator Mass Spectrometry  
30 Lawrence Livermore National Laboratory  
31 P.O. Box 808, L-397  
32 Livermore, CA 94550

35 \*Current address:

1 Virginia Polytechnic Institute and State University  
2 Department of Fisheries and Wildlife Sciences  
3 101B Cheatham Hall  
4 Blacksburg, VA 24061  
5  
6 Phone: (540) 818-4099  
7 Fax: (540) 231-7580  
8 Email: rleaf@vt.edu  
9

## 13 INTRODUCTION

15 The red abalone, *Haliotis rufescens* Swainson, supports an important recreational fishery in  
16 northern California and was once important commercially (Karpov et al. 2000). Because of  
17 historical depletions of *Haliotis* spp. populations in California (Karpov et al. 2000, Rogers-Bennett  
18 et al. 2002) there are concerns about the sustainability of the current fishery (California Department  
19 of Fish and Game, Marine Region 2005). Biological information, such as the age-at-length  
20 relationship, is a key parameter for the determination of management strategies and has only  
21 recently been described for red abalone in northern California by analysis of marked and  
22 recaptured individuals (Rogers-Bennett et al. 2007).

23 Although mark-recapture studies provide information about the age-at-length relationship,  
24 they can be limited in their ability to estimate the ages of large individuals. Age-at-length studies  
25 of northern California red abalone raised in aquaria indicate that the average size of the largest  
26 individuals in the population ( $L_{\infty}$ ) would be 170 to 236 mm MSL (maximum shell length) (Ault  
27 1985). Rogers-Bennett et al. (2007) reported  $L_{\infty}$  values of 254.2 mm MSL from individuals marked  
28 and recaptured at one site in northern California. However, red abalone exhibit asymptotic growth  
29 with a maximum recorded size of 313 mm MSL (Rogers-Bennett et al. 2007) and it is not  
30 uncommon for the lengths of individuals targeted in the recreational fishery to exceed the

published  $L_{\infty}$  values. Thus, it is not possible to use reported age-at-length relationships to estimate the ages for a component of the harvested population.

Methods that enable the determination of the ages of large individuals are necessary for the complete description of the age-at-length relationship of a species. Two strategies for directly estimating age-at-length for abalone are counting growth zones (discontinuous rings, marks, or lines in the shell) and analysis of seasonal stable isotope ratios in shell carbonate. Use of growth zone counts for age determination can be problematic: it has been documented that the formation of growth zones are irregular and may preclude consistent quantification (Forster 1967, Poore 1970, McShane & Smith 1992). Age estimation based on the ratio of stable isotopes in shell carbonate was successful at determining age and growth rates for a few mollusk species, including abalone (Cespuglio et al. 1999, Richardson 2000, Gurney et al. 2005). Oxygen isotopes are incorporated into shell carbonates in equilibrium with seawater and oxygen isotope ratios ( $^{18}\text{O}/^{16}\text{O}$ ) can be correlated with temperature, thereby providing a measure of temperature change as a proxy for seasonal change (Epstein et al. 1953). In addition, changes in the ratio of stable carbon isotopes ( $^{13}\text{C}/^{12}\text{C}$ ) can also provide a proxy for rate of shell formation by creating a record of seasonal productivity (Fairbanks & Dodge 1979, Krantz et al. 1984, Romanek et al 1987). The accuracy of these stable isotope methods for age determination is contingent upon the assumption that patterns in isotopic ratio change are indicative of annual growth. Analysis of stable isotopes has proven useful for determining early growth rates in ontogeny when growth rates are greatest, but the method is limited by the resolution of carbonate extraction techniques and cannot be performed at a resolution necessary to detect seasonal patterns in the older, slower growing parts of the shell (Romanek et al. 1987). Because of these limitations and assumptions, an independent chronometer for shell carbonate formation is desirable for accurate age and growth determination.

The use of the time-specific bomb-radiocarbon ( $^{14}\text{C}$ ) marker preserved in the carbonate structure of organisms is a promising method for validating age-at-length estimates (Campana 2001). Atmospheric testing of thermonuclear devices in the 1950s and 1960s greatly increased the naturally occurring levels of  $^{14}\text{C}$  in the atmosphere. Atmosphere-ocean gas exchange processes transferred bomb-derived  $^{14}\text{C}$  into the surface oceans and it was subsequently taken up and preserved in the carbonate structures of marine organisms residing in the mixed layer. Identification of the initial rise in bomb  $^{14}\text{C}$  in the carbonate structure of these organisms provides a chronological tool for determining age and growth. Successful applications of this technique range from validation of growth-zone derived estimates for invertebrates (Turekian et al. 1982, Weidman & Jones 1993) and fishes (Kalish 1993, Kerr et al. 2004, Piner & Wischniowski 2004) to the determination of growth rates and age when growth-zone derived age estimates were poor or not possible for invertebrates (Landman et al. 1988, Ebert & Southon 2003), algae (Frantz et al. 2000, 2005), and fishes (Andrews et al. 2005). In this study, a series of carbonate samples taken along the trajectory of growth from a single red abalone shell were analyzed for  $^{14}\text{C}$  to investigate the feasibility of using the time-specific bomb  $^{14}\text{C}$  marker to validate a red abalone age-at-length relationship.

## METHODS

One red abalone shell (251 mm MSL) was used in this study to investigate the feasibility of detecting  $\Delta^{14}\text{C}$  in red abalone shell and to assess the validity of competing VBGF estimates using the change in  $^{14}\text{C}$  due to atmospheric nuclear weapons testing ( $\Delta^{14}\text{C}$ ) recorded in shell material. The specimen analyzed in this study was collected in 1968, with an uncertainty of  $\pm 1$  y, from near the Gualala River, Mendocino, in northern California, USA. To prepare the shell for carbonate

1 extraction thin sections (approximately 2 mm wide) were removed perpendicular to the growth  
2 margin in multiple locations using a diamond bladed saw. Thin sections were mounted on glass  
3 slides with Cytoseal™ or wax. Four carbonate samples were extracted from the prismatic layer of  
4 the mounted thin sections using a New Wave® micromill with a 0.5 mm Brassler® drill bit.  
5 Extraction locations were based on preliminary VBGF predictions, described below, and were  
6 chosen to span the initial rise of the  $^{14}\text{C}$ -bomb pulse that is known to have occurred in surface  
7 ocean waters at  $1958 \pm 1$ . Because extractions from a single individual are necessarily  
8 autocorrelated we refer to each as a subsample. The first subsample was taken at 249 mm MSL,  
9 within 2 mm of the leading margin of growth, and three additional subsamples were taken at 227  
10 mm, 217 mm, and 75 mm MSL. The precision of extraction was  $\pm 0.5$  mm of the target sample  
11 location.

12         The extraction procedure produced small powdered fragments ( $\sim 5$  mg) that were weighed  
13 to the nearest 0.1 mg. For  $\Delta^{14}\text{C}$  analysis, calcium carbonate ( $\text{CaCO}_3$ ) was converted to  $\text{CO}_2$  and  
14 then to graphite (Vogel 1987) and measured for  $^{14}\text{C}$  content by accelerator mass spectrometry  
15 (AMS) at the Center for Accelerator Mass Spectrometry, Lawrence Livermore National  
16 Laboratory, Livermore, California, USA. The  $^{14}\text{C}$  measurements were reported as  $\Delta^{14}\text{C}$  values and  
17 an assumed  $\delta^{13}\text{C}$  value of zero was used in calculating the  $\Delta^{14}\text{C}$  values, which is representative of  
18 marine carbonates (Stuiver & Polach 1977). We tested for  $^{14}\text{C}$  contamination of the shell specimen  
19 and the workspace where carbonate extractions were performed. Alcohol soaked filter paper was  
20 rubbed on the shell and equipment ( $n = 4$ ). No  $^{14}\text{C}$  contamination was detected on any equipment  
21 or the shell specimen.

22         To estimate the dates of formation of extracted subsamples, three VBGF models were  
23 constructed based on tag-recapture data from northern California. These data were obtained from

899 tagged and recaptured red abalone at five sites in Sonoma and Mendocino counties from 1971 to 1978 (for details see Leaf et al. 2007). Only tagged red abalone at liberty for  $1 \text{ y} \pm 18 \text{ days}$  ( $\sim 5\%$  of  $1 \text{ y}$ ) within single or multiple year intervals were used for analysis. Individuals at liberty for a greater or lesser time period were excluded from VBGF parameter estimation because we suspected that growth for this species is not uniform throughout the year. Fabens' (1965) method was used to derive the VBGF parameter  $k$ , the growth rate constant,  $\text{y}^{-1}$ , and three  $L_{\infty}$  values, the average maximum size of an individual in the population (mm MSL), from the tag-recapture data using a non-linear curve fitting protocol in R (version 2.3.1).

$$L_{\text{recapture}} = L_{\text{tag}} + (L_{\infty} - L_{\text{tag}})(1 - e^{(-k \cdot \Delta t)}) \quad \text{Eq. 1}$$

The value of  $L_{\infty}$  was fixed in each of the three VBGF models to the maximum recorded size of the species (313 mm MSL) and two arbitrarily chosen sizes: 298 mm MSL and 283 mm MSL. Variables in the Fabens' equation (Eq. 1) are:  $L_{\text{recapture}}$ , the MSL (mm) of an individual at the time of recapture;  $L_{\text{tag}}$ , the MSL (mm) of an individual at the time of tagging; and  $\Delta t$ , the duration at liberty in years. In this formulation of the VBGF we assume that the age at size 0 mm ( $t_0$ ) is 0 y. A Ford-Walford plot (Walford 1946) was used to estimate  $k$  from the tag-recapture data to parameterize the non-linear curve-fitting algorithm. Confidence intervals (95%) of the mean value of  $k$  for each of the three candidate VBFG models were determined by Monte-Carlo sampling of randomized residual error values. The three von Bertalanffy growth functions were evaluated for goodness of fit by Akaike information criteria (AIC) and qualitatively to tag-recapture data using the growth vector method presented by Cailliet et al. (1992). AIC is a measure of the goodness of fit of competing models to data. The value  $\Delta_i$  is a measure of the fit of a model, model  $i$ , relative to that of the best fit model (the model with the lowest AIC value,  $\text{AIC}_{\text{min}}$ ) where  $\Delta_i = \text{AIC}_i - \text{AIC}_{\text{min}}$  (Burnham & Anderson 2002). Values of  $\Delta_i > 10$  indicate that the competing model has very little



support (Burnham & Anderson 2002). Growth vector analysis of the tag-recapture data was performed by anchoring growth vectors to the VBGF by assuming that the length at first capture corresponds to the age predicted by the VBGF. Growth vectors represent the change in time since first capture ( $\Delta t$ , y) and the change in length during the time at liberty ( $\Delta L$ , mm).

For each subsample extracted from the shell the back-calculated mean and range of the date of shell formation were determined based on estimates of growth from each of the three VBGF growth models. The range of the date of shell formation was calculated using the confidence interval associated with  $k$  from the VBGF, the incorporation of the uncertainty of the year of shell collection ( $1968 \pm 1$  y), and the incorporation of the width of the subsample extraction ( $\pm 0.5$  mm). Thus, the estimate of the earliest date of shell formation at each of the four subsample target locations, was estimated using the upper 95% confidence interval of  $k$ , an assumed date of shell collection of 1967, and a shell length given that the MSL is the minimum length sampled during extraction (subsample target  $- 0.5$  mm). The estimate of the most recent date of shell formation at each of the four subsample locations area was estimated using a small  $k$  value (the lower 95% confidence interval), an assumed collection year of 1969, and a shell length given that the MSL is the maximum length sampled during extraction (subsample target  $+ 0.5$  mm). The mean year of shell formation at a target area was estimated using the mean value of  $k$ , the median collection year of 1968, and the MSL at the target extraction point.

The fit of the candidate VBGF model estimates of the dates of shell subsample formation were evaluated qualitatively and through simulation. The estimate of the date of formation from each VBGF estimate of each subsample was compared with the  $\Delta^{14}\text{C}$  records for two regional reference  $\Delta^{14}\text{C}$  time series: yelloweye rockfish (*Sebastes ruberrimus*) (Kerr et al. 2004) and Pacific halibut (*Hippoglossus stenolepis*) (Piner & Wischniowski 2004). The temporal agreement

of the red abalone subsample series with these records were used as one basis for evaluation of the age and growth estimates from each of the VBGF trajectories. A simulation was also performed in which the precision of the three VBGF models to correctly predict the year of formation of the subsample formed at the inception of the radiocarbon rise was evaluated.

## RESULTS

The quality of each of the VBGF models to describe growth based on the tag-recapture data was variable. The VBGF, with a constrained  $L_{\infty}$  value of 313 mm MSL had a poor fit to the tag-recapture data ( $\Delta_i = 61.3$ ) relative to other models. This model had an estimate of  $k$  that indicated that growth ( $k = 0.0561 \text{ y}^{-1}$ , 95% CI: 0.0532 to 0.0589  $\text{y}^{-1}$ ) was less than half that predicted from the Ford-Walford estimate ( $k = 0.137 \text{ y}^{-1}$ ). The estimate of  $k$  increased in models with smaller  $L_{\infty}$  values and model fit was improved: the model with  $L_{\infty} = 298$  mm MSL had an estimated  $k = 0.0619 \text{ y}^{-1}$  (95% CI: 0.0618 to 0.0647  $\text{y}^{-1}$ ) and the fit to the data was improved ( $\Delta_i = 32.8$ ). The von Bertalanffy growth estimate with an  $L_{\infty}$  value of 283 mm MSL had the best fit to the tag-recapture data (AIC = 5864.2) and was predicted to have the greatest growth rate,  $k = 0.0689 \text{ y}^{-1}$  (95% CI: 0.0673 to 0.0705  $\text{y}^{-1}$ ). This best fit model resulted in a predicted age of the specimen to be 32 y with a range of 30 to 33 y. The distribution of observed growth, represented by the growth vectors, relative to the growth predicted by the VBGF for the best fit model, indicated that the predicted VBGF model underestimated growth of individuals smaller than 150 mm and overestimated growth of individuals larger than 150 mm (Figure 2). This pattern in the growth vectors was evident for each of the other candidate VBGF models.

There was a correspondence between the  $\Delta^{14}\text{C}$  values and VBGF age estimates from the red abalone specimen with each of the  $\Delta^{14}\text{C}$  reference time series' (Figure 1). The only red

abalone subsample with a clearly post-bomb  $\Delta^{14}\text{C}$  level was from the 249 mm MSL subsample ( $\Delta^{14}\text{C}\text{‰} = -16.8\text{‰} \pm 4.8$ ) (Table 1). This subsample had an estimated year of formation of 1966 to 1968, based on the three VBGF models, and had  $\Delta^{14}\text{C}$  values similar to yelloweye rockfish samples with estimated years of formation of 1964 ( $\Delta^{14}\text{C}\text{‰} = -22 \pm 3$ ) and 1965 ( $\Delta^{14}\text{C}\text{‰} = -7.4 \pm 3.1$ ). The subsample extracted at the 227 mm MSL location ( $\Delta^{14}\text{C}\text{‰} = -93.2 \pm 4.2$ ) was estimated to have been formed during the inception of the rise of the radiocarbon concentration in the northeastern Pacific (1959 to 1962) based on the three VBGF estimates (Table 1). The  $\Delta^{14}\text{C}\text{‰}$  value of this subsample was similar to samples from yelloweye rockfish with estimated years of formation of 1950 to 1963 and Pacific halibut samples estimated to have been formed in 1944 to 1958. The subsample taken from the 217 mm MSL location ( $\Delta^{14}\text{C}\text{‰} = -104.0 \pm 3.6$ ) had an estimated year of formation, based on VBGF estimates, of 1957 to 1960 (Table 1). The subsample extracted from the 217 mm MSL location had  $\Delta^{14}\text{C}\text{‰}$  that were most similar to samples from the yelloweye rockfish estimated to be formed in  $1944 \pm 2$  y and  $1956 \pm 2$  y and six samples from the Pacific halibut time series with estimated years of formation of 1947 to 1959. The subsample extracted from the 75 mm MSL location ( $\Delta^{14}\text{C}\text{‰} = -115.2 \pm 3.7$ ) was estimated to have been formed during 1936 to 1944 (Table 1).

The simulation of the three VBGF models resulted in a variable precision in their ability to estimate the date of formation of the subsample formed at 227 mm MSL. We assume this subsample to have been formed at 1959, the inception of the radiocarbon rise in the northeast Pacific. In order for the model with  $L_{\infty} = 313$  mm MSL to predict this year of formation of the 227 mm MSL subsample, the value of the  $k$  in the model could not exceed  $0.040 \text{ y}^{-1}$ . For the model with  $L_{\infty} = 298$  mm MSL to predict the year of formation of the 227 mm MSL subsample the value of  $k$  could not exceed  $0.050 \text{ y}^{-1}$ . In these two cases the expected value of  $k$  was outside the

1 predicted 95% confidence interval of the parameter. The value of  $k$  necessary for the model with  
2  $L_{\infty} = 283$  mm MSL to predict the date of formation of 1959 is  $0.068 \text{ y}^{-1}$  and this was the only  
3 model to precisely predict the date of formation of the 227 mm MSL subsample within the  
4 estimated 95% confidence interval of  $k$  ( $0.0673$  to  $0.0705 \text{ y}^{-1}$ ).  
5  
6

## 7 DISCUSSION

8 In this paper we show that red abalone shell material is a recorder of the regional temporal  
9 pattern of  $\Delta^{14}\text{C}$ ; the temporal trend of  $\Delta^{14}\text{C}$  levels measured in the abalone shell generally  
10 corresponded to both the yelloweye rockfish and Pacific halibut time series', and that the use of  
11  $\Delta^{14}\text{C}$  analysis of red abalone shell material can provide insight into the validity of VBGF estimates.  
12 We evaluated the fit of each candidate growth model with the tag-recapture data and in reference to  
13 its prediction of the year of the inception of the rise in radiocarbon. We found that the model that  
14 best described the tag-recapture data (the lowest AIC value) was the most reasonable at predicting  
15 the year of the subsample formed at the inception of the rise of radiocarbon in the northeast Pacific.

16 We conclude that the growth model with  $L_{\infty} = 283$  mm MSL and  $k = 0.0689 \text{ y}^{-1}$  (95% CI:  
17  $0.0673$  to  $0.0705 \text{ y}^{-1}$ ) provides the best fit of the three candidate models because this model  
18 predicts the date of formation of the critical 227 mm MSL subsample most precisely. It is unlikely  
19 that the 227 mm MSL subsample was formed in the early 1960's, as the two alternative growth  
20 models ( $L_{\infty} = 298$  mm MSL and  $L_{\infty} = 313$  mm MSL) predict because the corresponding VBGF  
21 growth rate constant ( $k \text{ y}^{-1}$ ) for each model would need to be very small ( $\leq 0.040$  or  $\leq 0.050 \text{ y}^{-1}$ ).  
22 The age of this specimen, predicted from the best fit curve is not younger than 32 y and could be

1 older. We note that this conclusion does not preclude the validity of a model parameterized with a  
2 value of  $L_{\infty}$  less than 283 mm MSL.

3 The temporal correspondence of  $\Delta^{14}\text{C}$  and the estimated ages of each red abalone  
4 subsample are similar to both of the regional time series' but there appears to be a slight shift  
5 toward more recent years of formation. Ambiguity in the date of specimen collection could result  
6 in this apparent shift: the uncertainty of  $\pm 1$  y for the collection year can explain the shift in the  
7 subsample series, if the shell was indeed collected in 1967. Because the subsample extracted at  
8 249 mm was 2 mm away from the leading margin of growth it may have formed as early as 1966.  
9 The measured  $\Delta^{14}\text{C}$  level for this subsample, when compared to the reference time series, provides  
10 support for this hypothesis. This subsample was important in the time series because it sets up the  
11 basis for projecting growth back to a birth year: it was clearly formed after the inception of the  $^{14}\text{C}$   
12 rise.

13 The VBGF parameters from the best fit model presented in this study are considerably  
14 different than those previously reported for red abalone. Ault (1985), using red abalone collected  
15 in northern California and maintained in aquaria, determined  $k$  values of  $0.11 \text{ y}^{-1}$  to  $0.19 \text{ y}^{-1}$ .  
16 Rogers-Bennett et al. (2007) reported VBGF parameter values of  $k = 0.108 \text{ y}^{-1}$  and  $L_{\infty} = 254.2 \text{ mm}$   
17 derived from 208 recaptures at a single location in northern California and included 38 tagged  
18 individuals that were 50 to 100 mm MSL when first tagged and were at liberty from eight to 16  
19 months. A subset of 23 individuals in this data were 5 to 30 mm MSL at first tagging. The VBGF  
20 estimates of the tag-recapture data used in this study, when analyzed using Fabens' method with an  
21 unconstrained  $L_{\infty}$  parameter value, resulted in VBGF estimates of  $k$  that were more similar to these  
22 published studies:  $k = 0.159 \text{ y}^{-1}$  (95% CI: 0.150 to  $0.168 \text{ y}^{-1}$ ) ( $L_{\infty} = 201.470 \text{ mm MSL}$ , 95% CI:  
23 198.1 to 204.9 mm MSL) than the values of  $k$  predicted in this study when  $L_{\infty}$  was constrained.

The differences between the  $k$  values reported in this work and those previously reported may be due to differences in the spatial and temporal growth dynamics of red abalone, the misspecification of VBGF model parameters, or misspecification of the von Bertalanffy growth model to describe the age-at-length relationship of this species in northern California. McShane et al. (1994) reported that significant differences in the mean length of *H. iris* populations in New Zealand are correlated to latitude and exposure. Variation in VBGF parameters among populations of *H. iris* are a result of differences in relative exposure (McShane & Naylor 1995) and it is likely that the fine scale variation in growth at different sites, which were combined in this study, has contributed to the low precision of the VBGF estimates. Temporal variation in growth trajectories of red abalone has been described in southern California by Haaker et al. (1998); it was suspected that growth is depressed during periods of increased water temperature and low productivity. Experimental work has supported this hypothesis (Vilchis et al. 2005). The misspecification of the arbitrarily chosen values of  $L_{\infty}$  may have also contributed to differences in the growth trajectories predicted by this and previously published studies: VBGF parameters  $k$  and  $L_{\infty}$  are strongly negatively correlated (Chen et al. 2003). The assignment of a large, arbitrary chosen  $L_{\infty}$  value will greatly influence the value of  $k$ . Finally, although the VBGF has been widely used to describe the age-at-length relationship of Haliotidae (Day & Fleming et al. 1992) it generally has a poor fit to abalone growth (Matsuishi et al. 1995) and alternative models have been used (Rogers-Bennett et al. 2007, Hancock 2004). The relatively consistent underestimation of growth of small ( $< 150$  mm MSL) and overestimation of growth of large ( $> 150$  mm MSL) red abalone observed in this study, as indicated by the vector method, may indicate that the VBGF may not be appropriate to describe the age-at-length relationship of this species in northern California (Figure 1).

Our work suggests that  $\Delta^{14}\text{C}$  dating can be applied in a more comprehensive study to determine the ontogenetic growth trajectory of red abalone, guide growth model specification, and growth model parameter selection. We recognize that making population level inferences from four autocorrelated subsamples, taken from a single individual, implies numerous assumptions including: the single specimen grew in a similar way to all northern California abalone, that  $^{14}\text{C}$  uptake is consistent throughout ontogeny, and that the age-at-length relationship derived from tag-recapture work from multiple sites from 1971 to 1978 is similar to that of the subsampled specimen collected in 1968 ( $\pm 1$  y) which had an estimated birth year of 1936. A strategy that consists of intensively subsampling a number of large similar sized red abalone shells with known dates of collection from the same area is necessary for a complete and unambiguous age and growth validation for this species in the region. The results of this study indicate that such an approach is promising. Although the tag-recapture work used in this study approximates a growth rate that is plausible, analysis of  $^{14}\text{C}$  allows for an alternate determination of growth rates and the determination of the maximum age of large individuals.

#### ACKNOWLEDGMENTS

We thank D. Ardizzone and L. Kerr for assistance in sample preparation and D. Shoemaker for providing the red abalone specimen used in this study. This work was supported by the Dr. Earl H. Myers and Ethel M. Myers Oceanographic and Marine Biology Trust of Pebble Beach, California, the National Sea Grant College Program of the U.S. Department of Commerce's National Oceanic and Atmospheric Administration under NOAA Grant number NA06RG0142, project number R/F-190, through the California Sea Grant College Program; and in part by the California State Resources Agency. This research was also supported by the Center for Accelerator Mass Spectrometry under the University Collaborative Research Program at Lawrence Livermore National Laboratory and was performed, in part, under the auspices of the U.S. Department of Energy by Lawrence Livermore National Laboratory under Contract No. FG/CE74/29PC495660

- 1 The views expressed herein do not necessarily reflect the views of any of those"qti cpl c wpu
- 2 The U.S. government is authorized to reproduce and distribute for governmental"r wtr qugu0"
- 3



## LITERATURE CITED

- Andrews, A.H., E.J. Burton, L.A. Kerr, G.M. Cailliet, K.H. Coale, C.C. Lundstrom & T.A. Brown. 2005. Bomb radiocarbon and lead-radium disequilibria in otoliths of bocaccio rockfish (*Sebastes paucispinis*): a determination of age and longevity for a difficult-to-age fish. *Mar. Freshw. Res.* 56:517-528.
- Ault, J.S. 1985. Some quantitative aspects of reproduction and growth of the red abalone, *Haliotis rufescens* Swainson. *J. World Maricul. Soc.* 16:398-425.
- Burnham, K. P., & D. R. Anderson. 2002. Model selection and multimodel inference: a practical information-theoretic approach. 2nd Edition. New York, New York: Springer-Verlag. 488 pp.
- Cailliet, G. M., H. F. Mollet, G. G. Pittenger, D. Bedford & L. J. Natanson. 1992. Growth and demography of the pacific angel shark (*Squatina californica*), based upon tag returns off California. *Aust. J. Mar. Freshw. Res.* 43:1313-30.
- California Department of Fish and Game, Marine Region. 2005. Abalone Recovery and Management Plan. 359 pp.
- Campana, S.E. 2001. Accuracy, precision and quality control in age determination, including a review of the use and abuse of age validation methods. *J. Fish Biol.* 59:197-242.
- Cespuglio, G., C. Piccinetti & A. Longinelli. 1999. Oxygen and carbon isotope profiles from *Nassa mutabilis* shells (Gastropoda): Accretion rates and biological behaviour. *Mar. Biol.* 135:627-634.
- Chen, Y., M. Hunter, R. Vadas & B. Beal. 2003. Developing a growth transition matrix for the stock assessment of the green sea urchin (*Stronglyocentrotus droebachiensis*) off Maine. *Fish. Bull.* 101:737-744.
- Day, R.W & A.E. Fleming. 1992. The determinants and measurement of abalone growth. In S. A. Shepherd, M. J. Tegner, & S. A. Guzmán del Prío, editors. Abalone of the World: Biology, Fisheries and Culture. Oxford: Fishing News Books. pp. 141-168.
- Ebert, T.A. & J.R. Southon. 2003. Red sea urchins (*Stronglyocentrotus franciscanus*) can live over 100 years: confirmation with A-bomb <sup>14</sup>carbon. *Fish. Bull.* 101:915-922.
- Epstein, S., R. Buchbaum, H.A. Lowenstam & H.C. Urey. 1953. Revised carbonate-water isotopic temperature scale. *Bull. Geol. Soc. Amer.* 64:1316-1326.
- Fabens, A.J. 1965. Properties and fitting of the von Bertalanffy growth curve. *Grow.* 29: 265-289.

- 1 Fairbanks, R.G. & R.E. Dodge. 1979. Annual periodicity of the  $^{18}\text{O}/^{16}\text{O}$  and  $^{13}\text{C}/^{12}\text{C}$  ratios in the  
2 coral *Montastrea annularis*. *Geochim. Cosmochim. Acta* 43:1009-1020.
- 3
- 4 Forster, G.R. 1967. The growth of *Haliotis tuberculata*: results of tagging experiments in  
5 Guernsey 1963-65. *J. Mar. Biol. Assoc. U.K.* 47: 287-300.
- 6
- 7 Frantz, B.R., M. Kashgarian, K.H. Coale & M.H. Foster. 2000. Growth rate and potential  
8 climate record of a rhodolith using  $^{14}\text{C}$  accelerator mass spectrometry. *Limnol. Oceanogr.*  
9 45:1773-1777.
- 10
- 11 Frantz, B.R., M.S. Foster, & R.Riosmena-Rodriguez. 2005. *Clathromorphum nereostratum*  
12 (Corallinales, Rhodophyta): The oldest alga? *J. Phycol.* 41:770-773.
- 13
- 14 Gurney, L.J., C. Mundy & M.C. Porteus. 2005. Determining age and growth of abalone using  
15 stable oxygen isotopes: a tool for fisheries management. *Fish. Res.* 72:353-360.
- 16
- 17 Haaker, P.L., D.O. Parker, K.C. Barsky & C.S.Y. Chun. 1998. Growth of red abalone, *Haliotis*  
18 *rufescens* (Swainson) at Johnsons Lee, Santa Rosa Island, California. *J. Shellfish Res.* 17:747-  
19 753.
- 20
- 21 Haaker, P. L., D. O. Parker, & K. C. Henderson. 1986. Red abalone size data from Johnsons Lee,  
22 Santa Rosa Island, collected from 1978 to 1984. Marine Resources Technical Report 53.
- 23
- 24 Hancock, A. T. 2004. The biology and fishery of Roe's Abalone *Haliotis roei* Gray in south-  
25 western Australia, with Emphasis on the Perth Fishery. Ph.D. Thesis, University of Western  
26 Australia.
- 27
- 28 Kalish, J.M. 1993. Pre- and post-bomb radiocarbon in fish otoliths. *Earth Planet. Sci. Lett.* 114:  
29 549-554.
- 30
- 31 Karpov, K. A., P. L. Haaker, I. K. Taniguchi, & L. Rogers-Bennett. 2000. Serial depletion and the  
32 collapse of the California abalone fishery. In: A. Campbell, editor. Workshop on rebuilding  
33 abalone stocks in British Columbia. *Can. Spec. Publ. Fish. Aquat. Sci.* 130:11-24.
- 34
- 35 Kerr, L.A., A.H. Andrews, B.R. Frantz, K.H. Coale, T.A. Brown, & G.M., Cailliet.  
36 2004. Radiocarbon in otoliths of yelloweye rockfish (*Sebastes ruberrimus*): A reference time  
37 series for the coastal waters of southeast Alaska. *Can. J. Fish. Aquat. Sci.* 61:443-451.
- 38
- 39 Krantz, D.E., D.S. Jones & D.F. Williams. 1984. Growth rates of the sea scallop, *Placopecten*  
40 *magellanicus*, determined from the  $^{18}\text{O}/^{16}\text{O}$  record in shell calcite. *Biol. Bull.* 167:186-199.
- 41
- 42 Landman, N.H., E.R.M. Druffel, J.K. Cochran, D.J. Conahue & A.J.T. Jull. 1988. Bomb-  
43 produced radiocarbon in the shell of the chambered nautilus: rate of growth and age at  
44 maturity. *Earth and Planet. Sci. Lett.* 89:28-34.
- 45

- 1 Leaf, R.T., Rogers-Bennett, L., & P.L. Haaker. 2007. Spatial, temporal, and size-specific variation  
2 in mortality estimates of red abalone, *Haliotis rufescens*, from mark-recapture data in  
3 California. *Fish. Res.* 83: 341-350.
- 4
- 5 Matsuishi, T., K. Saito & Y. Kanno. 1995. Growth curve of abalone. *Bull. Fish. Sci. Hokkaido*  
6 *Univ.* 46:53-62.
- 7
- 8 McShane, P. E., D. R. Schiel, S. F. Mercer, & T. Murray. 1994. Morphometric variation in *Haliotis*  
9 *iris* (Mollusca: Gastropoda): analysis of 61 populations. *N. Z. J. Mar. Freshw. Res.* 28:357-  
10 364.
- 11
- 12 McShane, P. E., & J. R. Naylor. 1995. Small-scale spatial variation in growth, size at maturity, and  
13 yield-and egg-per-recruit relations in the New Zealand abalone *Haliotis iris*. *N. Z. J. Mar.*  
14 *Freshw. Res.* 29:603-612.
- 15
- 16 McShane, P. E., & M. G. Smith. 1992. Shell growth checks are unreliable indicators of age of the  
17 abalone *Haliotis rubra* (Mollusca: Gastropoda). *Aust. J. Mar. Freshw. Res.* 43:1215-1219.
- 18
- 19 Piner, K. R. & S. G. Wischniowski. 2004. Pacific halibut chronology of bomb radiocarbon in  
20 otoliths from 1944 to 1981 and a validation of ageing methods. *J. Fish. Biol.* 64:1060-1071.
- 21
- 22 Poore, G.C. 1972. Ecology of New Zealand abalones, *Haliotis* species (Mollusca: Gastropoda) 3.  
23 Growth. *N. Z. J. Mar. Freshw. Res.* 6:534-559.
- 24
- 25 Richardson, C.A. 2000. Molluscs as archives of environmental change. *Oceanogr. Mar. Biol.*  
26 *Annu. Rev.* 39:103-164.
- 27
- 28 Rogers-Bennett, L., P.L. Haaker, T.O. Huff, & P.K. Dayton. 2002. Estimating baseline  
29 abundances of abalone in California for restoration. *Calif. Coop. Oceanic Fish. Invest. Rep.*  
30 43:97-111.
- 31
- 32 Rogers-Bennett, L., Rogers, D.W. & S. Schultz. 2007. Estimating growth and mortality parameters  
33 for red abalone (*Haliotis rufescens*) in northern California. *J. Shellfish Res.* 26:1-10.
- 34
- 35 Romanek, C.S., D.S. Jones, D.F. Williams, D.E. Krantz & R. Radtke. 1987. Stable isotopic  
36 investigation of physiological and environmental changes recorded in shell carbonate from the  
37 giant clam *Tridacna maxima*. *Mar. Biol.* 94:385-393.
- 38
- 39 Stuiver, M., & H.A. Polach. 1977. Discussion: reporting of  $^{14}\text{C}$  data. *Radiocarbon* 19:355-363.
- 40
- 41 Turekian, K.K., J.K. Cochran, & Y. Nozaki. 1982. Determination of shell deposition rates of  
42 *Artica islandica* from the New York Bight using natural  $^{228}\text{Ra}$  and  $^{228}\text{Th}$  and bomb-produced  
43  $^{14}\text{C}$ . *Limnol. Oceanogr.* 27:737-741.
- 44

- 1 Vilchis, L. I., Tegner, M. J., Moore, J. D., Friedman, C. S., Riser, K. L., Robbins, T.T., & P.K.  
2 Dayton 2005. Ocean warming effects on growth, reproduction, and survivorship of southern  
3 California abalone. *Ecol. App.* 15(2):469-480.  
4
- 5 Vogel, J.S., D.E. Nelson & J.R. Southon. 1987. <sup>14</sup>C Background levels in an accelerator mass  
6 spectrometry system. *Radiocarbon* 19: 323-333.  
7
- 8 Walford, L.A. 1946. A new graphic method of describing the growth of animals. *Biol. Bull. Mar.*  
9 *Biol. Lab. Woods Hole* 90: 141-147.  
10
- 11 Weidman, C.R. & G.A. Jones. 1993. A shell-derived time history of bomb <sup>14</sup>C on Georges Bank  
12 and its Labrador Sea implications. *J. Geophys. Res.* 98: 14577-14588.  
13

Table 1. Summary of estimated ages, dates of formation, and  $\Delta^{14}\text{C}\%$  for extracted samples.

Shell length at extraction (mm)	Estimated mean age and (range) years <sup>i</sup>	Estimated mean year and (range) of sample formation <sup>ii</sup>	Sample mass (mg)	$\Delta^{14}\text{C}\%$	$\pm$
249	31 (27 to 32)	1967 (1966 to 1968)	5.0	-16.8	4.8
227	24 (22 to 24)	1960 (1959 to 1963)	5.1	-93.2	4.2
217	21 (20 to 22)	1957 (1957 to 1961)	6.1	-104.0	3.6
75	4 (4 to 5)	1941 (1940 to 1945)	5.0	-115.2	3.7

- <sup>i</sup>. The estimated mean age was derived from the mean parameter estimate of the best fit von Bertalanffy model ( $L_{\infty}$ =283 mm MSL,  $k$ =0.0689  $\text{y}^{-1}$ ). The age range was derived from the absolute minimum and maximum age estimates of the three von Bertalanffy curves and incorporated the 95% confidence intervals of  $k$  of each curve and the width of the sample extraction (shell length at extraction  $\pm$  0.5 mm).
- <sup>ii</sup>. The mean year of sample formation was derived from the mean age estimate and an assumed date of shell collection of 1968. The range in year of sample formation was derived from the estimated range of ages and incorporated the variation in the estimated date of collection of the shell (1968  $\pm$  1 year).

## Figure legends

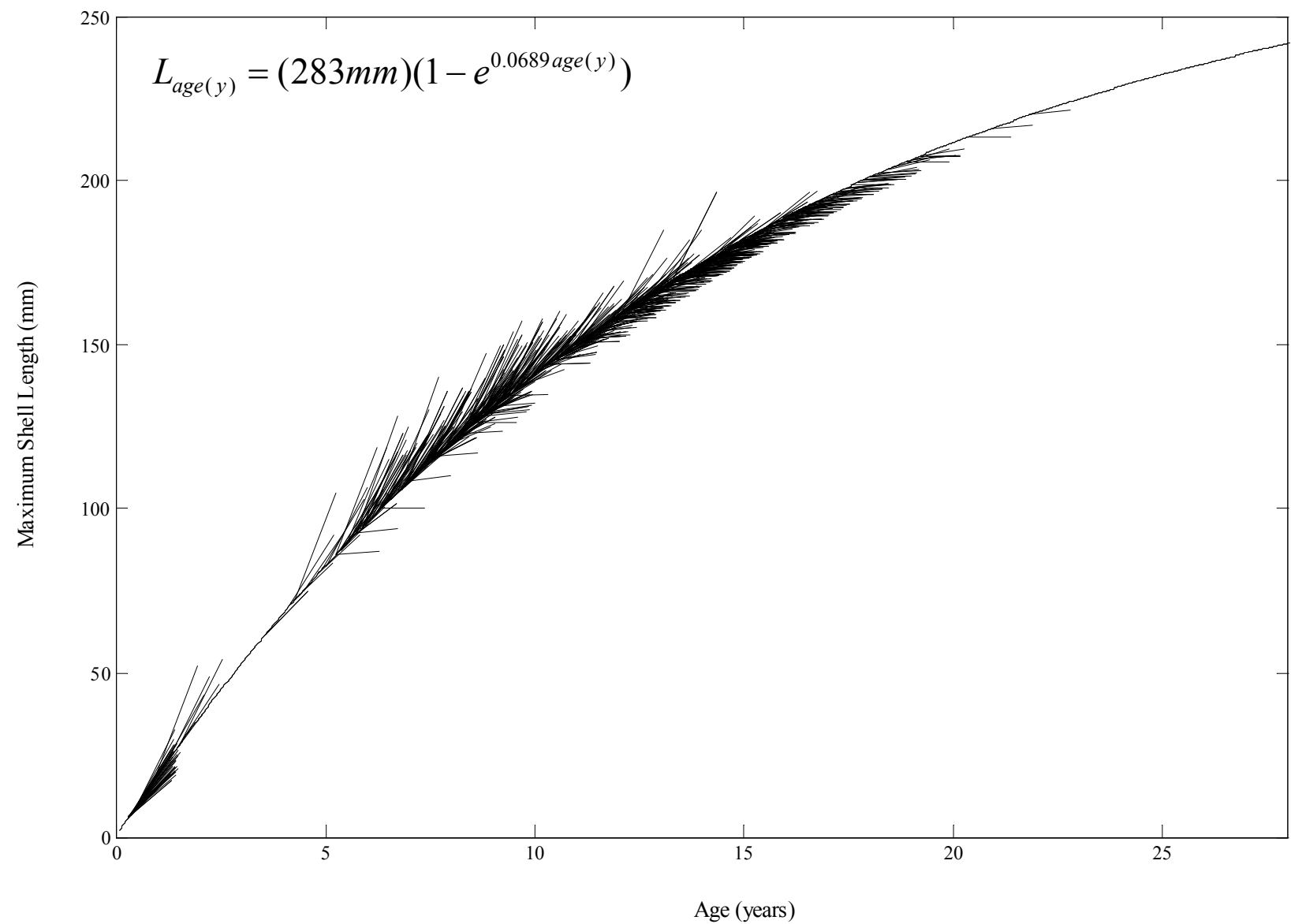
### Figure 1.

Tag-recapture growth vectors fit to the best fit Von Bertalanffy growth function ( $k = 0.0689 \text{ y}^{-1}$ ,  $L_{\infty} = 283 \text{ mm MSL}$ ). Growth vectors are anchored to the curve by assuming that the age at tagging is predicted by the VBGF. Vectors represent growth as the change in maximum shell length ( $\Delta\text{MSL}$ , mm) during time between tagging and recapture ( $\Delta$  years).

### Figure 2.

Radiocarbon values of red abalone subsamples extracted from a single individual in relation to their estimated mean formation dates based on the best fit von Bertalanffy growth curve ( $k = 0.0689 \text{ y}^{-1}$ ,  $L_{\infty} = 283 \text{ mm MSL}$ ) and two reference time series: southeast Alaska yelloweye rockfish (Kerr et al. 2004) and northeastern Pacific halibut (Piner and Wischniowski 2004).

Leaf et al.  
Bomb  $^{14}\text{C}$  and red abalone age and growth  
Figure 1.



Leaf et al.  
Bomb  $^{14}\text{C}$  and red abalone age and growth  
Figure 2.

